Supporting Information

Kang et al. 10.1073/pnas.1408315111

Site Selection

We selected abandoned oil and gas wells for measurement based on location information, access (legal and logistical), wellhead geometry above ground, land cover, geographic coverage, and plugging status. Site visits were made to confirm well locations and evaluate logistical access issues. Wells on both public lands and private properties were considered (Table S1). Private properties were only considered if the surface landowner granted access. (Flux chambers are designed to enclose and not touch the well, therefore, property owners need to give permission.) Although wells were mainly selected based on legal and logistical access, effort was made to ensure that measurements were made in regions with different land cover and that we had broad geographic coverage. Wells were also selected so that the numbers of measured plugged and unplugged wells were representative of abandoned wells in Pennsylvania (Fig. 1). The proportion of measured wells that are plugged, at 26% (Table S1), is similar to the proportion of wells that are plugged on the PA Department of Environmental Protection's list, which is 29%.

We measured 19 wells over five sampling rounds (Table S2) in McKean and Potter counties in PA. As of July 30, 2014, the number of abandoned oil and gas wells on the PA DEP's list of abandoned and orphaned oil and gas wells that are in McKean and Potter counties are 4,301 and 187 respectively, which correspond to 35% and 1.5% of total wells on the PA DEP's list. In fact, McKean County has the largest number of abandoned wells in Pennsylvania, followed by Venango County with 24% of total abandoned wells.

The measured wells were located on four different land cover types: grassland, wetland, river, and forest (Table S3). Five of the measured wells were located in the Allegheny National Forest. Nine were located on a 40-acre private property in Otto Township. The remaining two wells, one on a private property and one in the West Branch Tunungwant Creek, were in the City of Bradford. The three wells in Hebron Township, Potter County, were on two different private properties.

Although we have extrapolated emission results from 19 wells to the entire state of Pennsylvania, this was done only to show that the magnitude of the problem is significant relative to other methane sources. We recognize that the extrapolated number is highly uncertain. Quantifying this uncertainty is not possible given the available information. Information on the wells such as the date of drilling, completion, and abandonment and the target geologic formation are unavailable. We do not attempt to make any assumptions on the well attributes in this paper.

Nine of the 19 wells measured are on a 40-acre private property in Otto Township. Methane flow rates from these wells span three orders of magnitude and range from 0.9 to 210 mg/h/well. The large range of emission rates implies that close proximity does not necessarily imply similar flow rates. The mean and median of these flow rates are 57 and 12 mg/h/well, respectively, which is orders of magnitude lower than the average of 1.1×10^4 mg/h/well for all 19 wells. The nine wells on this property are not high emitters, and are not likely to bias the overall mean flow rate to be higher than presented.

On January 17, 2014, only 1 of the 19 measured wells was on the PA DEP's list; however, as of July 30, 2014, 7 of the 19 measured wells are on the PA DEP's list. All six additional wells are on the 40-acre private property in Otto Township. The seventh well on the PA DEP's list is a high emitter.

The selection of control locations was mainly based on site conditions. The distance between the control and the well is defined as the distance between the outer extent of the well (casing or cementing) and the outer edge of the flux chamber. For example, the control located 0.1 m from a well represents the integrated flux from 10 to 39 cm away from the outer edge of the well, based on the smallest flux chamber design. Although the control locations varied from 0.1 to 62 m from the measured well, most control locations were between 1 and 10 m from the measured well. Only 3 out of 42 control locations were 10 cm from the well. We have not determined a relationship between the horizontal distance from a well and methane fluxes from the soil, although we observed that flow rates from the controls were consistently orders of magnitude smaller than the average well flow rate. At most sites, only one or two controls were sampled. More measurements are necessary to determine if methane emissions from the surrounding soils are affected by the presence of an abandoned well.

Flux Chambers and Sampling

Chamber Design and Construction. A static chamber methodology was adapted from techniques to measure trace gas fluxes from soil–plant systems (1, 2). For well measurements, multiple-component chambers of various geometries were designed to enclose the wellhead and measure the emissions of methane and other trace gases from the well and the immediate surrounding area (Fig. S1). For controls, both single- and multicomponent chambers were designed. A schematic of the multiple-component chamber (Fig. S1) shows the distances, d and h_3, that separate the well from the chamber.

To accommodate different geometries of surface protrusions (e.g., well casing, monument/marker) and/or cement bases, we built four multiple-component chambers with the following footprints: circular with a 29-cm diameter (small), circular with 50-cm diameter (medium 1), circular with 55 cm (medium 2), and square with widths of 90 cm (large). The chamber heights were adjusted to accommodate surface protrusions and ranged from 0.23 to 2 m. The resulting flux chamber geometries were cylindrical and rectangular prismatic; 97% of measurements were performed using cylindrical chambers.

In the single-component chambers, vent tubes and sampling ports were installed through holes drilled in the rigid bucket. The multiple-component chamber has three major parts: collar, rigid frame, and bag. The chamber collars were made of prefabricated cylindrical buckets of rigid plastic material trimmed using a jigsaw or aluminum siding with grooves in which a tight bungee cord would be used to seal the collar and the bag (Fig. S1). Rigid frames were built to support the bag and form cylindrical or rectangular chambers. The frames were made of PVC pipe, rigid plastic, aluminum siding, and/or fence posts. Bags were made of 4-mm-thick polyethylene drop cloths and designed to snugly fit over the rigid frame and be airtight. Single-component chambers have a height of 25 cm and enclose volumes of 14–16 L depending on field conditions. Multiple-component chambers are larger and enclose volumes of 37–1,400 L.

At least one set of vent tubes and sampling ports was installed on each of the bags. Vent tubes made of Tygon laboratory tubing with 1/8″ (3.1 mm) inner diameter were installed on the top face of each chamber to transmit atmospheric pressure changes to the enclosed air volume. Tube lengths were ~1 m, which is more than a factor of 4 greater than minimum lengths recommended in ref. 1. Sampling ports with one-way Luer connections were created on the side of the chamber at approximately half the height of the chamber. The vent tubes and sampling ports were

installed on the chambers using bulkhead connectors, brass hose barbs, and Teflon tape.

To ensure sufficient mixing in these larger chambers, we installed closed-air circulation systems composed of one or more 12-volt DC cooling fans each powered by eight AA batteries in all multiple-component chambers. The fans and battery packs were installed on the rigid frame to maximize mixing inside the chamber.

Chamber Deployment. To obtain a snug fit, minimize soil disturbance, and limit air leakage, the single-component chambers and multiple-component chamber collars were placed in 1″ to 2″ grooves (h_1 in Fig. S1) in the soil. For multiple-component chambers, the rigid frames were placed on top of the collars, which were secured by PVC fittings, and enclosed within the chamber bag. The chambers were sealed around the collar with either a water lock or with tight bungee cords that fit into grooves around the collars. Chambers enclosing wells were installed around surface protrusions and in some cases, cement bases, and did not touch any material visibly associated with the well.

We also chose flux chambers based on magnitudes of the methane flux, based on previous measurements of the same location, if available, or visible signs of high flow rates such as bubbling. For high emitting wells, larger chambers were deployed to ensure that the chamber could be considered static and concentration changes could be measured at 5-min intervals. For low emitting wells, smaller chambers were used to minimize sampling duration and maximize mixing.

Sampling. Gas samples from chambers were collected in 20 mL Wheaton serum vials for gas chromatographic analysis and 150 mL Wheaton glass serum bottles or 0.5–3 L SamplePro FlexFilm air sample bags for isotopic analysis. Butyl rubber stoppers were used in all Wheaton vials and sealed with aluminum crimps. Used vials were flushed with more than 100 mL of ultra-high-purity nitrogen or air. All vials were flushed at least twice with ambient air or air zero and evacuated with a hand or mechanical pump to pressures of <10 kPa. We took 3–17 gas samples in 20 mL vials mainly at 5-, 10-, and 20-min intervals over durations of 20 min to 25 h depending on knowledge of the methane emissions from previous measurements or visible signs of high flow rates. For each sample, a 50-mL air sample was extracted from the chamber using a 60-mL syringe, which was then transferred to a vial, using a needle, or directly to a bag. To minimize contamination, syringes were flushed at least 10 times before use in a new chamber and at least 5 times between samples taken at different times from the same chamber. We also took one 150 mL, 0.5 L, or 3 L sample from the chambers for isotopic measurements at the end of each measurement period. Throughout the sampling period, the pressure in the chamber was maintained at atmospheric pressure through a vent tube, which was tested occasionally with a flow meter. The samples in glass bottles were analyzed within 3 (4) weeks of collection for alkane (isotope) concentrations.

Uncertainties. Uncertainties associated with flux chamber design, deployment, and sampling arise from uncertainties in effective chamber volume, incomplete chamber sealing, altered diffusion gradients, equipment contamination, temperature and pressure effects, and microbial activity. Many of these uncertainties bias the calculated flow rates to be lower than actual values.

Uncertainties in effective chamber volume can arise due to the flexibility of the bag material, insufficient mixing inside the chamber, and neglecting connected pore space in soils. To determine the chamber volume, we assumed that the chamber was a cylinder, an elliptic cylinder, or a rectangular/trapezoidal prism. However, both the rigid frame and the bag may deviate from these standard volumes due to equipment damage, and site and environmental conditions. The deviations are most likely in terms of the horizontal area of the multicomponent chambers, which has a flexible component. Based on this assumption the error can range from −32 to 23%, assuming a 5-cm deviation for the smallest multicomponent chamber and a 10-cm deviation for the large rectangular chamber. Insufficient mixing inside the chamber may lead to a smaller effective volume and nonuniform concentration distributions inside the chamber. This is especially of concern in large chambers. The large multiple-component chambers may contain zones where the circulation system does not provide sufficient mixing. These zones are more likely to be present in corners of rectangular chambers and regions blocked by surface protrusions. To test mixing in the large rectangular chambers, we created two sampling ports on opposite sides of the chamber and samples were taken simultaneously from these ports. The sample results show that the error is 12% or less for five out of six samples and 44% for one of the samples. In addition, the effective chamber volume can be larger than the volume of the chamber aboveground because it can include the volume of air space belowground, specifically the connected air-filled voids in soil and the air space in the unplugged well. Effective volumes are generally calculated using tracers and such studies have shown that the larger effective chamber volumes due to void space in soil can lead to a 30% underestimate in fluxes (3). Furthermore, the depth to water surface of unplugged wells varies significantly; the deepest water surface in a measured well was ∼180 m. There have not been any studies of effective chamber volumes in such cases. The air space in unplugged wells can only lead to larger effective chamber volumes and lower chamber concentrations and flow rates.

Additional sources of uncertainties likely to bias the methane flow rates toward underestimation are air leakage due to imperfect seals and altered diffusion gradients. The leakage through imperfect seals (e.g., between chamber bag and collar), the vent tube, and any damaged zones of the chamber can also lead to an underestimation of flow rate. It is very difficult to quantify air leakage but we estimate that it is within 20% for random error of static chambers (4). After chamber deployment, the concentration of the chamber headspace increases, lowering the concentration gradient that is driving any diffusive flux. The altered diffusion gradient can lead to an underestimation of flux by up to 15% in soils without wells (5). This is mainly a concern for methane flow rates at controls where diffusive processes are more likely to govern. At high emitting wells, diffusive flow rates are likely to play a minor role. In locations with positive methane flow rates, which include all wells and some controls, this altered diffusion gradient biases the flow rate to be low.

In all three high emitting wells, we visually observed bag inflation during the sampling period. This signals the potential for two major sources of errors: an underestimate of effective chamber volume, and significant leakage such that the chamber can no longer be considered static. In both cases, the measured flow rates would be biased low.

Equipment contamination can occur when syringes, needles, chambers, and sample containers (glass vials, butyl rubber stoppers, or bags) exposed to high concentrations at a previous site are insufficiently flushed before use at another site. Contamination is a concern in this study because very wide ranges of concentrations can accumulate in the chambers. To minimize contamination, we flushed syringes 5–10 times before use in a new site, we did not use the same needle for more than one flux chamber, and we had dedicated flux chambers for measurements at control locations. Quantifying error due to contamination is difficult; however, any contamination would bias the flow rates to be low.

We did not have any temperature controls for the chamber and assumed that any temperature variations during chamber deployment (which was usually less than an hour) were small. We also focused on data collected from the first 20–81 min of chamber deployment and any later data were used only if their inclusion led to small changes in flux values. Any changes in

atmospheric pressure were assumed to be sufficiently transmitted through the vent tube and were assumed to be small.

Microbial activity is a concern in the chamber during deployment and sampling. Soil microbial communities can either produce CH_4 through methanogenesis or consume CH_4 via methanotrophic metabolisms, and the rates of these processes are a complex function of temperature, soil moisture, soil type, and other environmental variables (6). In general, saturated soils will be anaerobic, and CH_4 sources and unsaturated upland soils will be CH_4 sinks. As expected, control measurements in wetland areas produced the greatest CH_4 flow rate of 8.2 mg/h/location. Forest and grassland soils produced CH_4 at significantly lower rates than wetland soils, and in some cases, were CH_4 sinks due to methane oxidation. Methane oxidation in soils enclosed with wells inside chambers would further bias the fluxes low by consuming a portion of the methane emitted by the wells.

Analysis

Alkane Concentration. C_1–C_4 light hydrocarbons, including CH_4, C_2H_6, C_3H_8, and n-C_4H_{10}, were analyzed using flame ionization gas chromatography (GC) on a Shimadzu GC-2014 instrument. The carrier gas was ultra-high-purity helium, and hydrocarbon gases were separated on a 10-foot packed Porapak-Q column with a temperature program that involves a 2-min isothermal period at 100 °C followed by a temperature ramp of 10 °C per minute to 150 °C. The flame ionization detector was held at 200 °C. Air samples were extracted from the vials into a glass syringe, equilibrated to atmospheric pressure, and injected into the instrument via a sample loop. Air samples were discarded when the volume extracted into the syringe was less than 5 mL Instrument precision based on triplicate injections of a 1.00% methane standard is 2% for the July/August 2013 samples, 8% for October 2013 samples, and 2% for January 2014.

Peak identification in the sample chromatograph was accomplished by comparing retention times to those in the chromatograms of premixed gas standards from AirLiquide. These standards were used to develop calibration curves for each gas. The calibration curves were obtained using linear regression of the peak areas and the mixing ratios of the premixed standards, with the intercept set to zero. For methane, we used standards at 2.04 ppmv, 5 ppmv, 50 ppmv, 122 ppmv, 2,527 ppmv, 1%, and 100%. Based on this calibration information, the methane concentrations observed in the chamber ranged from 0.82 ppmv to 52%. For C_2–C_4 alkanes, we used three standards with ethane, propane, and n-butane concentrations of 5 ppmv, 50 ppmv, and 1%. The 5 and 50 ppmv standards also contained i-butane and were only available for the January 2014 samples. The objective for measuring the C_2–C_4 alkanes was to determine their presence and their concentrations relative to methane so that we can gain insight on the source of methane. Detection is defined qualitatively by the shape of the peak, relative to the baseline, and a minimum peak area of 100 mV·min. Alkane presence at a well or control location was noted when alkanes were detected in at least two samples. For these locations, the average ratio of the C_2–C_4 alkane with respect to methane was calculated.

Isotopic Composition. To measure the C isotopic composition of CH_4, a near-IR CW-CRDS was used. This system consists of three distributed feedback laser diodes, two of which were tuned to the absorption line peaks of $^{12}CH_4$ and $^{13}CH_4$ at 6,112 and 6,049 cm^{-1}, respectively, and a third that measured the baseline at 6,051 cm^{-1}. The multiple-laser design provides long-term stability of the system and increases the data-acquisition rate. The acquisition frequency was further increased by using a semiconductor optical amplifier to initiate cavity ring-down events. Optical isolators and spacing and orientation of optical elements were all used to prevent any Etalon effects. The optical cavity has a length of 0.653 m with one pair of super mirrors with reflectivities of over 99.9993% at a wavelength of 1.651 μm. This is equivalent to a 93.3-km absorption path length. A heat controller stabilized the temperature of the cavity at 30 ± 0.02 °C. The high repetition rate combined with the superhigh reflectivity mirrors and long-term temperature stability assures the high precision isotopic measurements of CH_4 near ambient methane concentration. The system has a detection limit of 1.9×10^{-12} cm^{-1} corresponding to 10 pptv of CH_4 at 100 Torr. CH_4 gas isotopic standards that have been analyzed by isotope ratio mass spectrometers were used to calibrate the CRDS. The $\delta^{13}C$-CH_4 values were reported relative to Viena Peedee Belemnite standard. For ambient air samples that contained 1.9 ppmv CH_4 the precision of the $\delta^{13}C$ of the CH_4 is ±1.7‰ (7). The 25 cc samples were equilibrated with the evacuated cavity to a pressure of 100 Torr to reduce peak overlaps between CO_2, H_2O, and $^{12}CH_4$ absorption peaks. A Nafion/Ascarite trap was used to remove H_2O vapor and CO_2.

Flow Rate Calculation

Mass flow rates F, in units of mass per time per well, were calculated using linear regression in *MATLAB* on the concentration data, c [mass/volume], over time, with the slope of the line then multiplied by the chamber volume to give the flow rate:

$$F = \frac{dc}{dt} \cdot V_e, \qquad \text{[S1]}$$

where dc/dt is the slope of the fitted line and V_e is the effective chamber volume. Concentration data were collected starting at the moment of chamber deployment. At least three data points, each representing different times, were used in the linear regressions. For most flow rates, five to seven data points were used. We assumed that the volumes of surface protrusions were small relative to the chamber volume. For control locations, flow rates were scaled based on the land areas covered by the chamber for the control and the nearest well location as follows:

$$F_{control,scaled} = F_{control,raw} \cdot \frac{A_{well}}{A_{control}}, \qquad \text{[S2]}$$

where $F_{control,scaled}$ is the methane flow rate scaled to the area of the well [mass/time/well], $F_{control,raw}$ is the methane flow rate of the control before scaling [mass/time/control], A_{well} is the ground surface area of the chamber at the well [length^2], and $A_{control}$ is the ground surface area of the chamber at the control [length^2]. We report flow rates of methane only. Flow rates of C_2–C_4 alkanes are not presented here because there are insufficient numbers of ethane, propane, and n-butane detections to calculate flow rates in most locations. Also, we have low confidence in the C_2–C_4 alkane concentrations because a standard in the range of most samples was not available at the time of the July, August, and October 2013 sampling campaigns.

In several chambers, changes in concentration declined with time during the sampling duration. This decline in methane accumulation could be because the chamber could no longer be considered static or due to altered diffusion gradients. For these flow rate measurements, data from the earlier time points where the relationship is linear and more representative of the flow rate at the time of chamber deployment, and less likely to be affected by altered concentration gradients, were used. Data from the first 10–81 min were used for 88% of the flow rates. The sampling duration was based on an assumed magnitude of the flow rates, with longer durations used for smaller flow rates.

The goodness of fit obtained by linear regression was evaluated with the R^2 value. Here, R^2 values greater than 0.8 were assumed to lead to a good flow rate estimate. However, flow rates with low R^2 values were not discarded here because this would lead to biased results that favor higher flow rates (8). R^2 values corre-

sponding to the measured methane flow rates are correlated with the absolute value of the flux with low R^2 values associated with smaller flow rates (Fig. S2). Therefore, P values (null hypothesis: flow rate = 0) were calculated and flow rates were set to zero for P values greater than 0.2. This resulted in 2 of the measurements at wells and 12 measurements at controls having zero flow rates. The two zero-flow rate measurements at wells correspond to one of three measurements made at each of the two wells, which were sampled over three sampling campaigns; the other two flow rate measurements at these two locations are positive and nonzero.

Flow rates were discarded if there was clear evidence of contamination. Evidence for contamination is determined by considering the sequence of sampling and equipment use, concentrations observed at the last location of equipment use, and comparisons of flow rates to other measurements and published values. A total of 3 flow rate measurements out of a total of 97 measurements were discarded.

Fluxes from controls were compared with published values. Over half of the methane fluxes from control locations are representative of fluxes found in other areas with similar land cover. In contrast, of the measured fluxes at well locations, 90% are 1–8 orders of magnitude greater than methane fluxes observed in other areas with similar land cover but without wells (9–11). It is important to note that the control locations may also be affected by the presence of the well; however, we have not investigated this thoroughly.

Error Estimation

We synthesized the key sources of uncertainties from flux chambers and sampling, laboratory analysis, and flux calculations to estimate the error in methane flow rate and emissions estimates. We assumed any source of uncertainty that is difficult to quantify contributes to the ±20% generally accepted random error for static chambers (non-steady-state) in natural environments without abandoned wells (4, 5). By summing the above error estimates, we estimated that the combined effect of the various sources of uncertainties in flow rate estimates leads to errors within a factor of two of our estimate. This precision is sufficient given the orders of magnitude variations in measured flow rates.

Methane Emission Estimates

Emissions were scaled up for the state of Pennsylvania using the mean methane flow rate from the 19 wells as the emission factor (0.27 kg/d/well) and an estimated 300,000–500,000 abandoned oil and gas wells as the activity. Fourteen out of the nineteen measured wells were measured 2–5 times. To represent the methane emission factor for a given well on an annual basis, the average of the multiple measurements at each well was used as the value for that well. The PA DEP has records of 12,127 abandoned, orphaned, and plugged oil and gas wells as of January 17, 2014. However, estimates of the number of abandoned oil and gas wells range from 300,000 to 500,000 in various reports by the PA DEP (Table S4). We note that the objective of this paper was to understand the emission factor and not to determine the number of wells.

The total anthropogenic methane emissions for Pennsylvania in 2010, estimated by the World Resources Institute (WRI) (as available in their Climate Analysis Indicators Tool) (12), is 15.26 Mt CO_2e per year (0.73 Mt CH_4 per year). WRI uses a global warming potential (GWP) of 21 following the second assessment report of the Intergovernmental Panel on Climate Change (12). The use of this GWP does not impact our percentages because they are in terms of mass of methane. The WRI estimates are uncertain and may underestimate total statewide GHG emissions (including CO_2) by a few Mt CO_2e per year (12). Furthermore, there are year-to-year variabilities. Considering the period from 2000 to 2010, the minimum and maximum methane emission estimates are 13.48 and 17.98 Mt CO_2e per year (12).

We also used gross natural gas withdrawals for Pennsylvania to consider the relative importance of methane emissions from abandoned oil and gas wells. In 2010, the natural gas withdrawal was 572,902 million cubic feet according to the US Energy Information Administration (EIA). There was a large increase in natural gas production in PA in 2011—1,310,592 ft^3 (also from the EIA). Nonmethane hydrocarbons and other gases are included in these natural gas withdrawal numbers, whereas our emissions estimates include only methane. If we include the nonmethane hydrocarbons emissions from abandoned wells, our emission estimates will be larger than reported here. We report methane emissions from abandoned oil and gas wells in terms of 2010 and 2011 production because we use 2010 when comparing with WRI estimates and 2011 production is used in the recent study on methane emissions from natural gas production sites (13).

1. Livingston G, Hutchinson G (1995) *Enclosure-Based Measurement of Trace Gas Exchange: Applications and Sources of Error. Methods in Ecology*, eds Matson P, Harriss R (Blackwell Science Ltd., Oxford), pp 14–51.
2. Reid MC, Tripathee R, Schäfer KVR, Jaffé PR (2013) Tidal marsh methane dynamics: Difference in seasonal lags in emissions driven by storage in vegetated versus unvegetated sediments. *J Geophys Res Biogeosciences* 118:1802–1813.
3. Rayment MB (2000) Closed chamber systems underestimate soil CO_2 efflux. *Eur J Soil Sci* 51:107–110.
4. Jassal RS, Black TA, Nesic Z, Gaumont-Guay D (2012) Using automated non-steady-state chamber systems for making continuous long-term measurements of soil {CO2} efflux in forest ecosystems. *Agric For Meteorol* 161:57–65.
5. Davidson E, Savage K, Verchot L, Navarro R (2002) Minimizing artifacts and biases in chamber-based measurements of soil respiration. *Agr For Meteorol* 113:21–37.
6. Le Mer J, Roger P (2001) Production, oxidation, emission and consumption of methane by soils: A review. *Eur J Soil Biol* 37:25–50.
7. Chen Y, et al. (2013) Measurement of the $^{13}C/^{12}C$ of atmospheric CH_4 using near-infrared (NIR) cavity ring-down spectroscopy. *Anal Chem* 85(23):11250–11257.
8. Savage K, Davidson EA, Richardson AD (2008) A conceptual and practical approach to data quality and analysis procedures for high-frequency soil respiration measurements. *Funct Ecol* 22:1000–1007.
9. Mosier A, Schimel D, Valentine D, Bronson K, Parton W (1991) Methane and nitrous oxide fluxes in native, fertilized and cultivated grasslands. *Nature* 350:330–332.
10. Altor AE, Mitsch WJ (2006) Methane flux from created riparian marshes: relationship to intermittent versus continuous inundation and emergent macrophytes. *Ecol Eng* 28:224–234.
11. Mander Ü, et al. (2010) Assessment of methane and nitrous oxide fluxes in rural landscapes. *Landsc Urban Plan* 98:172–181.
12. WRI CAIT 2.0 (2013) Climate Analysis Indicators Tool: WRI's Climate Data Explorer. Washington, DC: World Resources Institute. Available at cait2.wri.org.
13. Allen DT, et al. (2013) Measurements of methane emissions at natural gas production sites in the United States. *Proc Natl Acad Sci USA* 110(44):17768–17773.

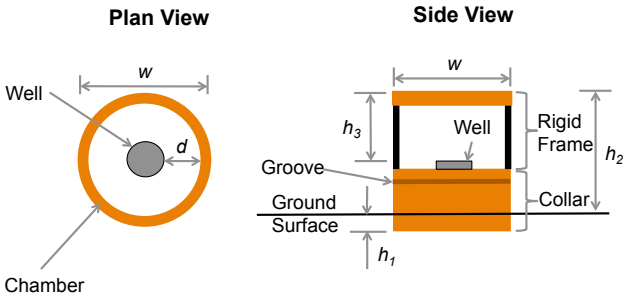

Fig. S1. Schematic of flux chamber collar and frame enclosing surface protrusions of an abandoned oil and gas well. All variables other than the chamber diameter, *w*, depend on location.

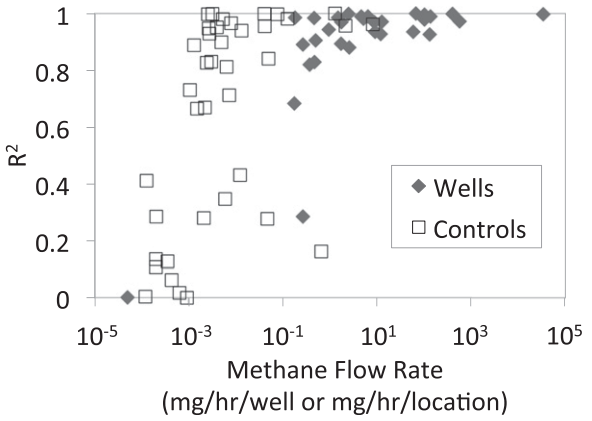

Fig. S2. The R^2 value for the linear regression and the corresponding methane flow rates.

Table S1. Summary of measured wells

			Number of wells	
Location	County	Ownership	Unplugged	Plugged
Allegheny National Forest	McKean	Public	2	3
City of Bradford	McKean	Private	1	0
City of Bradford	McKean	Public	1	0
Otto Township	McKean	Private	7	2
Hebron Township	Potter	Private	3	0
Total			14	5

Table S2. Summary of sampling campaigns

	Number of flow rate measurements		Average of mean daily temperatures over the sampling round (°C)	Locations
Sampling campaigns	Wells	Controls		
July 17–18, 2013	1	0	24	Otto Township
July 24–25, 2013	5	3	13	Otto Township
July 31–August 1, 2013	8	11	17	Otto Township
October 8–11, 2013	13	23	11	Otto Township, City of Bradford, Allegheny National Forest
January 26–31, 2014	14	15	−12	Otto Township, City of Bradford, Allegheny National Forest, Potter County

Table S3. Summary of measurements by land cover

	Number of locations/wells	
Land cover	Controls	Wells
Forest	23	9
Grassland	10	5
River	1	1
Wetland	8	4
Total	42	19

Table S4. Estimates of the number of abandoned oil and gas wells in Pennsylvania

Month	Year	Number of wells	Notes	Source Title	Created by
April	2000	325,000	Approximate	Pennsylvania's Plan for Addressing Problem Abandoned Wells and Orphaned Wells	PA DEP, Bureau of Oil and Gas Management Bureau of Oil and Gas Management
August	2012	350,000–500,000*	Wells drilled	Oil and Gas Technical Advisory Board Meeting Minutes	PA Oil and Gas Technical Advisory Board
March	2013	350,000	Estimated lower limit	Oil and Gas Well Drilling and Production in Pennsylvania	PA DEP
n/a	n/a	300,000	Estimate	The Well Plugging Program	PA DEP

*There are 10,921 active and inactive wells on the PA DEP list as of March 1, 2014. This would bring the number of abandoned oil and gas wells to 340,000–490,000 but we take the number here as is, assuming these are order of magnitude estimates.